

Rapid Communications

Rapid Communications are intended for the accelerated publication of important new results and are therefore given priority treatment both in the editorial office and in production. A Rapid Communication in Physical Review B should be no longer than four printed pages and must be accompanied by an abstract. Page proofs are sent to authors.

Critical behavior of the electron-spin-resonance linewidth in multilayered $\text{Cu}_{0.89}\text{Mn}_{0.11}/\text{Cu}$ spin glasses

D. L. Leslie-Pelecky and J. A. Cowen

*Department of Physics and Astronomy and Center for Fundamental Materials Research,
Michigan State University, East Lansing, Michigan 48824*

(Received 17 December 1991; revised manuscript received 21 July 1992)

The temperature dependence of the electron-spin-resonance linewidth, $\Delta H(T)$, has been measured in multilayered $\text{Cu}_{0.89}\text{Mn}_{0.11}/\text{Cu}$ as a function of spin-glass layer thickness W_{SG} with $1 \text{ nm} \leq W_{\text{SG}} \leq 500 \text{ nm}$. We find that the critical behavior, as characterized by the divergence strength C and exponent κ changes systematically with W_{SG} . A function parametrized in terms of the ratio of the freezing temperature in a sample with spin-glass layer thickness W_{SG} to that of the bulk, $T_f(W_{\text{SG}})/T_f(\infty)$, describes all data with $W_{\text{SG}} \geq 7 \text{ nm}$. Samples with $W_{\text{SG}} \leq 3 \text{ nm}$ do not obey this form and are better described by a two-dimensional form that diverges as $T^{-2.5}$. A universal function describing a crossover from three-dimensional to two-dimensional behavior as the layer thickness changes is suggested. Once the dependence of the critical part of $\Delta H(T)$ on $T_f(W_{\text{SG}})$ is known, finite-size and droplet relationships can be used to infer the dependence on W_{SG} . The possibility that this crossover is due to increasing anisotropy as W_{SG} is decreased is briefly discussed.

Interpretation of electron-spin-resonance (ESR) investigations of bulk spin glasses above T_f (Refs. 1–5) has been challenging. This is due in part to the nature of ESR measurements, which are made at high (GHz) frequencies and large (1–6 kG) magnetic fields, and in part to the very complicated behavior of spin glasses in the temperature range where they cannot be considered simple, noninteracting paramagnets, but are not yet frozen into a macroscopic spin-glass phase.

Static^{6,7} and frequency dependent^{8,9} susceptibility measurements of multilayered spin glasses have shown that the freezing temperature $T_f(W_{\text{SG}})$ decreases with decreasing spin-glass layer thickness, W_{SG} . The reduced freezing temperature, given by

$$\epsilon = [T_f(\infty) - T_f(W_{\text{SG}})] / T_f(\infty),$$

measures this depression relative to the bulk freezing temperature, $T_f(\infty)$. Standard finite-size scaling theory predicts that ϵ is proportional to $W_{\text{SG}}^{-1/\nu}$. Multilayers with $W_{\text{SG}} > 20 \text{ nm}$ confirm these predictions,^{6–9} with $\nu = 1.0 \pm 0.1$ (for $\text{Cu}_{0.89}\text{Mn}_{0.11}/\text{Cu}$) and $T_f(W_{\text{SG}})$ extrapolating to zero at $W_{\text{SG}} \approx 3 \text{ nm}$. Finite-size scaling fails for samples with $W_{\text{SG}} < 20 \text{ nm}$ and these data are indicative of crossover behavior from three to two dimensions, as shown within a droplet model.^{10–12} Experimental measurements show that $T_f(W_{\text{SG}})$ remains finite at even a single monolayer thickness.¹³

The ESR linewidth, $\Delta H(T)$, in bulk samples has been shown^{1–3} to decrease linearly with decreasing tempera-

ture for $T \gg T_f$. As T_f is approached, the linewidth diverges as a power law in reduced temperature, $t = (T - T_f)/T_f$. By measuring $\Delta H(T)$ as a function of W_{SG} , we hope to determine if the finite size and dimensionality effects that have been well documented in measurements of $T_f(W_{\text{SG}})$ are evident in the ESR linewidth and to use the results of this study to better understand the interpretation (and thus the utility) of this technique as applied to spin glasses.

Fabrication and characterization techniques have been previously reported⁷ and only details particular to this experiment are included here. UHV dc sputtering is used to interlayer $\text{Cu}_{0.89}\text{Mn}_{0.11}$ of layer thickness W_{SG} ($1 \text{ nm} \leq W_{\text{SG}} \leq 500 \text{ nm}$) with 30-nm buffer layers of Cu. The Cu interlayers prevent magnetic interactions between spin-glass layers. Films are mounted on flattened quartz rods for measurement in a Varian 4500 spectrometer at 9 GHz. To avoid Dysonian line shapes,¹⁴ the total sample thickness is limited to 500–700 nm, which is approximately $\frac{3}{4}$ of the skin depth. $T_f(W_{\text{SG}})$ was determined from SQUID susceptibility measurements at 100 G with a measuring time of about 300 sec per point.

First derivative line shapes are collected by computer as the temperature is lowered from 300 K to near $T_f(W_{\text{SG}})$ and are fit to a sum of real and imaginary parts of the susceptibility.¹⁵ The ratio of real to imaginary part is held constant for all temperatures and layer thicknesses. Residual impurities from the substrate give rise to a background, which is accounted for in the fitting procedure.

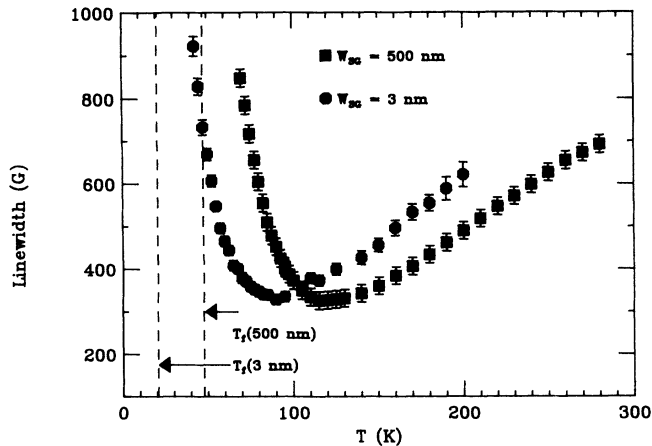


FIG. 1. The ESR linewidth as a function of temperature, $\Delta H(T)$, for $W_{SG}=500$ nm (squares) and 3 nm (circles). The freezing temperatures are indicated by dashed lines.

$\Delta H(T)$ in bulk spin glasses above T_f has been analyzed¹⁻³ in terms of Eq. (1)

$$\Delta H(T) = A + BT + Ct^{-\kappa}. \quad (1)$$

At high temperatures, $\Delta H(T)$ approaches a straight line characterized by the residual width A and the thermal broadening coefficient B . As T nears T_f , the linear behavior combines with a power law divergence in the reduced temperature t having divergence strength C and exponent κ .

Figure 1 shows $\Delta H(T)$ for samples with $W_{SG}=500$ nm (squares) and 3 nm (circles). Freezing temperatures are indicated by dashed lines. $\Delta H(T)$ can be fit to Eq. (1) for all samples studied ($1 \text{ nm} \leq W_{SG} \leq 500 \text{ nm}$) with the minimum linewidth approximately constant for all layer thicknesses; however, the position of the minimum linewidth changes from $2.4T_f(W_{SG})$ in the thick samples to $6.5T_f(W_{SG})$ in the 1-nm sample. The parameters obtained by fitting these data to Eq. (1) are summarized in Table I. The error in κ is ± 0.1 for all samples. The reduced temperature t is calculated using the value of $T_f(W_{SG})$ obtained from susceptibility measurements.

TABLE I. Parameters obtained by fitting $\Delta H(T) = A + BT + Ct^{-\kappa}$, with $t = [T - T_f(W_{SG})]/T_f(W_{SG})$. Values shown in parentheses for κ are from fits to the corresponding $T_f=0$ form.

W_{SG} (nm)	$T_f(W_{SG})$ (K)	A (G)	B (G/K)	C (G)	κ
500	47.5	-245 ± 15	3.36 ± 0.03	328 ± 13	1.50
100	47.5	-245 ± 14	3.46 ± 0.04	324 ± 17	1.50
50	45.0	-234 ± 14	3.47 ± 0.06	364 ± 16	1.60
30	42.5	-223 ± 14	3.51 ± 0.06	446 ± 16	1.80
10	35.0	-210 ± 14	3.60 ± 0.06	652 ± 13	2.00
7	31.0	-198 ± 18	3.74 ± 0.07	896 ± 17	2.15
3	20.5	-120 ± 19	3.80 ± 0.09	1182 ± 21	1.7 (2.55)
1	10.5	-70 ± 21	4.17 ± 0.12	2745 ± 63	1.8 (2.50)

Previous studies of Cu-Mn/Cu multilayers^{8,9} have demonstrated that samples with $W_{SG} \leq 5$ nm are more appropriately described by two-dimensional (2D) expressions. For the ESR linewidth, the 2D expression is obtained by replacing t in Eq. (1) with T and renormalizing the divergence strength. Fitting to this form does not appreciably change A and B . The renormalized divergence strength is not directly comparable with C and is not shown. The values of κ obtained from fitting to this form are shown in parentheses in Table I. Parameters for both forms were obtained by fixing κ , letting the other three parameters vary, and repeating the process. The best fit is determined by minimizing χ^2 .

All parameters show systematic trends as a function of layer thickness. The behavior of the residual linewidth implies a change in the Curie constant with W_{SG} . The increase in B with decreasing W_{SG} indicates an opening of the ESR bottleneck¹⁶ via the introduction of additional relaxation paths as a result of either the multilayered structure or the finite thickness of the samples. These phenomena will be addressed in a future publication, and we will instead focus on the critical behavior described by $\Delta H(T)^{ex} = \Delta H(T) - A - BT$. Both the divergence strength C and the exponent κ increase with decreasing layer thickness. κ has a value of 1.5 in the bulk [in agreement with that found in bulk AgMn (Ref. 1) and a theoretical prediction¹⁷] and increases to a value of 2.5 ± 0.1 in the thinner samples (with $T_f=0$).

The form of the dependence of the freezing temperature on W_{SG} has been shown^{8,9} to vary in different regimes. To avoid this complication, we have parametrized the data in terms of $T_f(W_{SG})/T_f(\infty) = 1 - \epsilon$. [Once this is done, the dependence of $\Delta H(T, \epsilon)$ on layer thickness can then be inferred from finite-size and droplet relationships in the appropriate regimes.] Figure 2 shows the divergence strength $C(T_f(W_{SG}))$ as a function of $\log_{10}[T_f(W_{SG})/T_f(\infty)]$. For samples with $W_{SG} \geq 7$ nm,

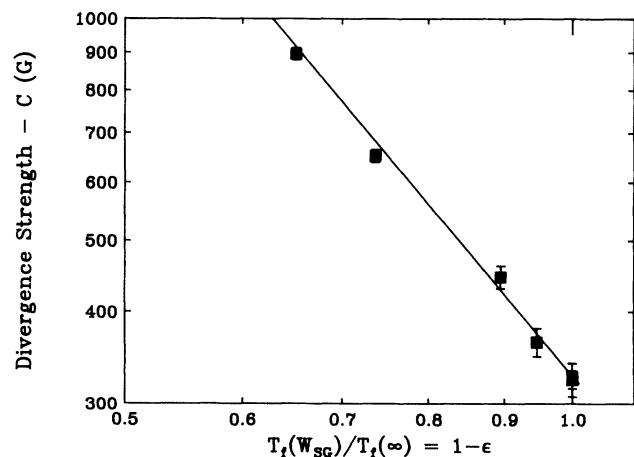


FIG. 2. The logarithm of the divergence strength $C(T_f)$ of a sample with freezing temperature T_f as a function of $\log_{10}(1 - \epsilon)$, with $\epsilon = T_f(W_{SG})/T_f(\infty)$. The solid line represents $C(T_f) = C(T_f(\infty))(1 - \epsilon)^{-a}$ [Eq. (2)] with $a = 2.4 \pm 0.1$.

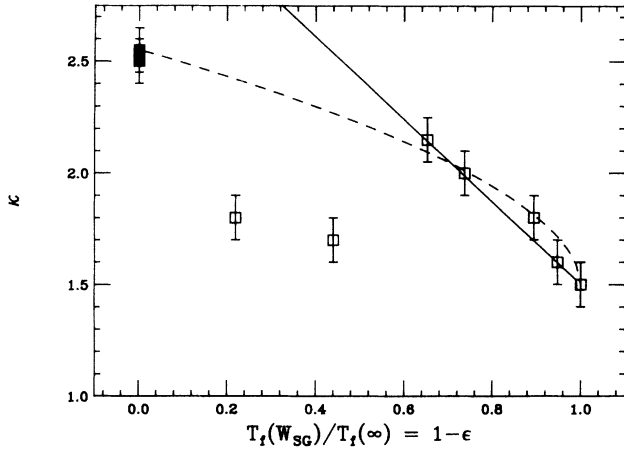


FIG. 3. The exponent κ as a function of $1 - \epsilon = T_f(W_{SG})/T_f(\infty)$. The solid boxes shown for $W_{SG} = 3$ and 1 nm are those obtained from fitting with $T_f = 0$. (See Table I.) Open boxes are values from fits to finite T_f . The solid line represents Eq. (3a) ($\kappa = 1.5 + b\epsilon$) with $b = 1.85 \pm 0.15$ and the dashed line represents Eq. (3b) ($\kappa = 1.5 + b'\epsilon^c$) with $b' = 1.05 \pm 0.04$ and $c = 0.54 \pm 0.05$.

the divergence strength follows the power law given by Eq. (2):

$$C(T_f(W_{SG})) = C(T_f(\infty)) \left[\frac{T_f(W_{SG})}{T_f(\infty)} \right]^{-a}$$

$$= C(T_f(\infty))(1 - \epsilon)^{-a}, \quad (2)$$

where $C(T_f(\infty))$ is the value of the divergence strength in the bulk and the exponent a has the value 2.4 ± 0.1 .

Figure 3 shows the exponent κ as a function of $T_f(W_{SG})/T_f(\infty)$, with the $T_f = 0$ values shown for the two thinnest samples. We can write κ as the sum of the bulk value, $\kappa(T_f(\infty))$, plus an additional part which describes the dependence on T_f . For samples with $W_{SG} \geq 7$ nm, the exponent κ obeys a straight line:

$$\kappa(T_f(W_{SG})) = \kappa(T_f(\infty)) + b \left[1 - \left[\frac{T_f(W_{SG})}{T_f(\infty)} \right] \right]$$

$$= \kappa(T_f(\infty)) + b\epsilon, \quad (3a)$$

where $\kappa(T_f(\infty)) = 1.5$ and $b = 1.85 \pm 0.15$; however, this predicts a value of $\kappa = 3.3$ for $T_f = 0$. One possible modification to Eq. (3a), which results in a more appropriate 2D limit is

$$\kappa(T_f(W_{SG})) = \kappa(T_f(\infty)) + b' \left[1 - \left[\frac{T_f(W_{SG})}{T_f(\infty)} \right] \right]^c$$

$$= \kappa(T_f(\infty)) + b'\epsilon^c \quad (3b)$$

with $b' = 1.05 \pm 0.04$ and $c = 0.54 \pm 0.05$. Equation (3b) is shown as a dashed line in Fig. 3. This modification, along with Eq. (2), results in a universal expression for $\Delta H(T, \epsilon)$ that describes a crossover from 3D to 2D behavior as $T_f(W_{SG})$ decreases. Note that the values of $T_f(W_{SG})$ used in fitting $\Delta H(T, \epsilon)$ are obtained at 100 G

and a measuring time of 300 sec, while the ESR measurements are over much shorter time scales and larger magnetic fields. Cumulative field and frequency effects on $T_f(W_{SG})$ might be more significant in thinner samples and clarification of how κ behaves as $T_f \rightarrow 0$ may require consideration of these effects.

We are not aware of any measurements or theoretical predictions for a 2D value of κ in metallic spin glasses. Our measured value of $\kappa = 2.5$ agrees with the general observation of $\kappa \geq 2$ found for two-dimensional antiferromagnetic Mn-Br and Mn-Cl salts¹⁸ fit using the measured Néel temperature. $\Delta H(T)$ has been measured on thin ferromagnetic films,¹⁹ but analysis of data above T_c has not been published. A percolation theory²⁰ developed to explain the ESR behavior of $\text{Rb}_2\text{Mn}_x\text{Mg}_{1-x}\text{F}_4$, a dilute two-dimensional antiferromagnet, predicted that $\Delta H(T)$ would diverge as $T^{-4.5}$, but the observed divergence was weaker.

A divergent ESR linewidth is seen in spin glasses, two-dimensional antiferromagnets, linear chain antiferromagnets,^{21,22} and in anisotropic three-dimensional ferromagnets and antiferromagnets.^{23,24} The only instances in which the ESR linewidth does not diverge are in cubic antiferromagnets such as RbMnF_3 and KMnF_3 , where $\Delta H(T)$ instead narrows near the Néel temperature.²⁵ Theoretical calculations of the ESR linewidth in antiferromagnets have emphasized the necessity of anisotropy in obtaining a divergence.^{25,26}

The anisotropy responsible for the diverging ESR linewidth in spin glasses was originally thought to be dipolar,³⁻⁵ however, Mozurkewich *et al.*¹ identified the Dzyaloshinskii-Moriya (DM) anisotropy as the dominant mechanism in Sb-doped Ag-Mn by showing that κ increases with increasing anisotropy. (Note that Sb doping also decreases the freezing temperature.) The similarity between the increase in κ with increasing anisotropy and decreasing W_{SG} raises the equation of how anisotropy is affected by reducing W_{SG} . If these changes are coupled, our measurements indicate that the anisotropy increases with decreasing W_{SG} ; whether this is due to an enhancement of the DM anisotropy or a change in the character of the exchange interaction is unknown. A number of experimental²⁷⁻³⁰ and theoretical³¹⁻³³ studies have investigated the importance of anisotropy to spin glass ordering in the bulk. Additional investigation of the relationship between W_{SG} and anisotropy is required to answer this question.

Further understanding and interpretation of the ESR linewidth divergence by comparison to other spin-glass measurements is hampered by the inability to relate exponents obtained from ESR measurements to other measured and theoretically calculated values. Wu, Mozurkewich, and Orbach² cite two calculations relating κ to $z\nu$: $\kappa = z\nu$ and $\kappa = z\nu - 2\beta$. These formulas predict values of $z\nu$ from 1.5 to 2.5 for the bulk, in agreement with those found by field and frequency scaling of $\Delta H(T)$.^{2,34} Measurements of $z\nu$ by susceptibility experiments in metallic⁷ and other spin glasses,^{35,36} as well as theoretical calculations^{37,38} consistently find values of $z\nu$ in the range of 6–10. Attempts to identify the value of κ in the nominally 2D case with other (2D) exponents is

similarly unsatisfying. The questions of why divergences are seen in one-dimensional magnets—which theoretically should not support long-range order—and why $\Delta H(T)$ departs from power-law behavior at relatively high ($t=0.6$) reduced temperatures also remain unanswered.

In summary, we have reported the first measurements of the ESR linewidth as a function of temperature in multilayered $\text{Cu}_{0.89}\text{Mn}_{0.11}/\text{Cu}$ spin glasses with spin-glass layer thicknesses from 1 to 500 nm. Although all samples follow the same qualitative form, systematic changes in the parameters describing the linewidth are seen. A single function in terms of $\epsilon = [T_f(\infty) - T_f(W_{\text{SG}})] / T_f(\infty)$ describes the linewidth for all samples with $W_{\text{SG}} \geq 7$ nm. Samples with $W_{\text{SG}} \leq 3$ nm are more appropriately fit with a two-dimensional form that diverges as $T^{-2.5}$. These two regimes describe a crossover from three-dimensional to two-dimensional behavior, and one

form for this crossover has been suggested. Similarity between the behavior of κ with increasing anisotropy and decreasing W_{SG} raises the possibility that decreasing W_{SG} increases the anisotropy. Further understanding of the ESR linewidth requires better knowledge of the magnetic field and frequency effects on $T_f(W_{\text{SG}})$, reconciliation of critical exponents with those from other types of experiments, theoretical calculation of κ in two dimensions and the clarification of the role of anisotropy.

The authors wish to thank R. Orbach, P. M. Duxbury, Norman O. Birge, and Jack Bass for helpful discussions and comments on this paper. The authors gratefully acknowledge support via NSF Grant No. DMR 8819429, the Center for Fundamental Materials Research at Michigan State University, and Rockwell International (D.L.L.-P.).

-
- ¹George Mozurkewich, J. H. Elliot, M. Hardiman, and R. Orbach, *Phys. Rev. B* **29**, 278 (1985).
²Wei-yu Wu, George Mozurkewich, and R. Orbach, *Phys. Rev. B* **31**, 4557 (1985).
³M. B. Salamon and R. M. Hermann, *Phys. Rev. Lett.* **41**, 1506 (1978).
⁴M. B. Salamon, *Solid State Commun.* **31**, 781 (1979).
⁵M. B. Salamon, *J. Magn. Magn. Mater.* **15-18**, 147 (1980).
⁶G. G. Kenning, J. M. Slaughter, and J. A. Cowen, *Phys. Rev. Lett.* **64**, 5781 (1988).
⁷G. G. Kenning *et al.*, *Phys. Rev. B* **42**, 2393 (1980).
⁸P. Granberg *et al.*, *J. Appl. Phys.* **67**, 5252 (1990).
⁹L. Sandlund *et al.*, *Phys. Rev. B* **40**, 869 (1989).
¹⁰Daniel S. Fisher and David A. Huse, *Phys. Rev. B* **36**, 8937 (1987).
¹¹D. S. Fisher and D. A. Huse, *Phys. Rev. B* **38**, 373 (1988).
¹²D. S. Fisher and D. A. Huse, *Phys. Rev. B* **38**, 386 (1988).
¹³L. Hoines, R. Stubi, R. Loloee, J. A. Cowen, and J. Bass, *Phys. Rev. Lett.* **66**, 1224 (1991).
¹⁴F. Dyson, *Phys. Rev.* **98**, 349 (1955).
¹⁵G. E. Pake, *Paramagnetic Resonance* (Benjamin, New York, 1962).
¹⁶S. E. Barnes, *Adv. Phys.* **30**, 801 (1981), and references therein.
¹⁷D. L. Huber, *Phys. Rev. B* **31**, 4420 (1985).
¹⁸R. D. Willett and M. Extine, *Phys. Lett.* **44A**, 503 (1973).
¹⁹Yi Li and K. Baberschke, *Phys. Rev. Lett.* **68**, 1208 (1992).
²⁰W. M. Walsh, Jr., R. J. Birgeneau, L. W. Rupp, Jr., and H. J. Guggenheim, *Phys. Rev. B* **20**, 4645 (1979).
²¹R. E. Dietz *et al.*, *Phys. Rev. Lett.* **26**, 1186 (1971).
²²T. T. P. Cheung *et al.*, *Phys. Rev. B* **17**, 1266 (1978).
²³R. H. Taylor, *Adv. Phys.* **24**, 681 (1971), and references therein.
²⁴Mohindar S. Seehra, *J. Appl. Phys.* **42**, 1290 (1973).
²⁵Mohindar S. Seehra, *Phys. Rev. B* **6**, 3186 (1972).
²⁶D. L. Huber, *Phys. Rev. B* **6**, 3180 (1972).
²⁷L. R. Walker and R. E. Walstead, *J. Magn. Magn. Mater.* **31-34**, 1289 (1983).
²⁸J. D. Reger and A. P. Young, *Phys. Rev. B* **37**, 5493 (1987).
²⁹A. Fert *et al.*, *J. Phys. (Paris)* **49**, 1173 (1988).
³⁰N. de Courtenay, H. Bouchiat, H. Hurdequint, and A. Fert, *J. Appl. Phys.* **61**, 4097 (1987).
³¹A. J. Bray and L. Viana, *J. Phys. C* **16**, 4679 (1983).
³²S. A. Roberts and A. J. Bray, *J. Phys. C* **15**, L527 (1982).
³³D. M. Cragg and D. Sherrington, *Phys. Rev. Lett.* **49**, 1190 (1982).
³⁴H. Mahdjour *et al.*, *Z. Phys. B* **63**, 351 (1986).
³⁵P. Svedlindh *et al.*, *J. Appl. Phys.* **63**, 4351 (1988).
³⁶E. Vincent and J. Hammann, *J. Phys. C* **20**, 2659 (1987).
³⁷A. T. Ogielski, *Phys. Rev. B* **32**, 7384 (1985).
³⁸R. P. Singh and S. Chakravarty, *Phys. Rev. Lett.* **57**, 245 (1986).